CCT-WG5 on radiation thermometry

Uncertainty budgets for realisation of scales by radiation thermometry

Joachim Fischer (PTB), Mauro Battuello (IMGC), Mohamed Sadli (BNM-INM), Mark Ballico (CSIRO), Seung Nam Park (KRISS), Peter Saunders (MSL), Yuan Zundong (NIM), B. Carol Johnson (NIST), Eric van der Ham (NMi/VSL), Wang Li (NMC/SPRING), Fumihiro Sakuma (NMIJ), Graham Machin (NPL), Nigel Fox (NPL), Sevilay Ugur (UME), Mikhail Matveyev (VNIIM)

Contents

1. Scope

Some recent international comparisons [1,2] and the preliminary results of the key comparison CCT-K5 [3] showed that the realisation of the ITS-90 above the freezing point of silver and its dissemination with tungsten strip lamps may be less straightforward than expected. In many cases, the deviations of the local realisations were higher than the combined estimated uncertainties. On the other hand, it must be considered that the realisation of the ITS-90 by radiation thermometry is a complex exercise involving a large number of operations and with many influencing parameters.

As the text of the ITS-90 [4] allows different methods and working wavelengths to be adopted, uncertainties may increase considerably in scale comparison exercises. For example, large additional uncertainties, up to some tenths of a degree may originate from referring the working wavelengths of the various laboratories to an agreed reference wavelength. The key comparisons (KC) require new approaches for the treatment of the uncertainties. For example, a conflict could originate between the uncertainties reported in the Appendix B (results of the KCs) and in Appendix C (list of the CMCs) of the MRA. *May the uncertainty of a CMC be lower than that reported in the Appendix B ? How can a lower uncertainty be supported by the results of a KC?*

The following paragraphs present an analysis of the base-line parameters underlying the scale realisation with respect to their contribution to the uncertainty budget. The paper is a joint effort of the working group on radiation thermometry of the Consultative Committee for Thermometry (CCT) summarizing the knowledge and experience of all experts in this field.

2. Uncertainty budget

Basically, we should distinguish between two different situations, i.e., the realisation of the ITS-90 and the comparison of scales by means of transfer standards.

The text of the ITS-90 states:

> Above the freezing point of silver the temperature T_{90} is defined by the equation:
>
> $$\frac{L_\lambda(T_{90})}{L_\lambda[T_{90}(X)]} = \frac{\exp(c_2[\lambda T_{90}(X)]^{-1}) - 1}{\exp(c_2[\lambda T_{90}]^{-1}) - 1} \qquad (1)$$
>
> where T_{90}(X) refers to any one of the silver {T_{90}(Ag)=1234.93 K}, gold {T_{90}(Au)=1337.33 K} or copper {T_{90}(Cu)=1357.77 K} freezing points, $L_\lambda(T_{90})$ and $L_\lambda[T_{90}(X)]$ are the spectral concentrations of the radiance of a blackbody at the wavelength (in vacuo) λ at T_{90} and at T_{90}(X) respectively, and c_2=0.014388 m·K.

No particular methods or wavelengths are recommended and consequently many approaches may be followed and different wavelengths may be adopted. In the past, and still today in some cases, the scale was maintained on tungsten strip lamps and the radiation thermometer was simply used as a flux comparator. Presently, the availability of highly stable detectors, e.g., the silicon photodiode, allows a direct calibration of the thermometer in terms of output signal versus temperature to be done. Traditionally, values of working wavelength in the range from 650 nm to 665 nm are selected. The choice of different wavelengths does not influence the uncertainty estimations of each laboratory in their own realisation of the scale, but may originate very high additional uncertainty contributions when a normalisation to a reference value must be done, as in the case of a comparison. This can occur because of the nature of the transfer artifact, which has a dependence of the emissivity with wavelength.

Two different analyses for the formulation of the appropriate uncertainty budgets will be done for the scale realisation and for the comparison.

2.1 Uncertainty budget for a scale realisation

Whichever method is adopted , the realisation of the ITS-90 above the freezing point of silver (1234.93 K) requires three basic operations to be carried out:

- **fixed-point calibration**
  this operation allows a value proportional to T_{90}(X) of equation (1) to be established;

- **spectral characterisation of the thermometer**
  knowledge of the response curve allows the value of λ in eq. (1) to be derived;

- **measurement of system non-linearity**
  knowledge of non-linearity, if any, allows radiance ratios to be measured correctly.

Basically, three different operational schemes can be devised for maintaining the ITS-90:

scheme 1:
- the fixed-point calibration is transferred to a reference tungsten strip lamp; this implies the determination of a current value on the lamp corresponding to a radiance temperature equal to the fixed-point temperature;
- a series of temperatures T_{90} are established and maintained on the lamp by measurement of radiance ratios; if necessary, the radiance ratios are adjusted for the non-linearity of the thermometer; this leads to the availability of a series of current and radiance temperature values; a polynomial interpolation equation can be calculated to relate temperature to current in a continuous way

scheme 2:
- the fixed-point calibration is transferred to a reference tungsten strip lamp;
- temperatures T_{90} of any source are determined according to the defining equation of the ITS-90 by measuring the signal ratios between the source at T_{90} and the reference lamp at the fixed-point temperature; if necessary, the signal ratios are adjusted for the non-linearity of the thermometer.

scheme 3:
- the fixed-point calibration is maintained on the thermometer. The output signal is assumed to be representative of T_{90}(X);
- a series of temperatures T_{90} are established as a function of the output signals of the thermometer. Signal ratios with respect to T_{90}(X) are calculated and, if necessary, adjusted for the non-linearity of the thermometer.

Table A Appropriate uncertainty components for each scheme

Source of uncertainty		Scheme 1	Scheme 2	Scheme 3
Fixed-point calibration	Impurities			
	Emissivity			
	Temperature drop			
	Plateau identification			
	Repeatability			
Spectral responsivity	Wavelength			
	Reference detector			
	Scattering, Polarisation			
	Repeatability of calibration			
	Drift			
	Out-of-band-transmittance			
	Interpolation and Integration			
Output signal	SSE			
	Non-linearity			
	Drift			
	Ambient conditions			
	Gain ratios			
	Repeatability			
Lamp	Current			
	Drift, Stability			
	Base and ambient temperature			
	Positioning			
	Polynomial fit			

The three schemes for the realisation and maintenance of the ITS-90 give rise to different uncertainty budgets but with many common uncertainty components. Table A associates with each scheme the appropriate uncertainty components by filling a grey cell. For the dark grey cells see 3.1.

The individual uncertainty components are analysed below. When values of uncertainty are reported, they apply for an effective wavelength of 650 nm and are referred to the gold point; i.e., the reference temperature

throughout this paper is T_{90}(X) = 1337.33 K. Two categories of uncertainty are introduced, a) normal and b) best, referring to uncertainties that a) can be easily obtained at present in national metrology institutes, and b) can be obtained with considerable effort by the small number of leading workers in the field [29]. In all tables always standard uncertainties are quoted.

2.1.1 Uncertainty in the fixed-point calibration

2.1.1.1 Impurities

Generally, samples whose purity ranges from 99.999% (5N) to 99.9999% (6N) are used. There are no definite indications of differences in the fixed-point temperatures in using purer samples, as the results are dependent on the nature and the distribution of the impurities inside the sample. Experimental investigations on the effects of impurities for the Ag and Cu points can be found in [5-7]. Differences of less than 10 mK have been found between 5N and 6N Ag samples. A detailed analysis with references on the influence of impurities can also be found in [8].

Uncertainty budget (Impurities):

quantity X_1	estimate x_1	standard uncertainty $u(x_1)$		probability distribution	sensitivity coefficient c_1	uncertainty contribution $u_1(y)$			
						at T_{ref}		at 3000 K	
		normal value	best value			normal value	best value	normal value	best value
∂ impurity	0	10 mK	5 mK	normal	$(T/T_{ref})^2$	10 mK	5 mK	50 mK	25 mK

2.1.1.2 Emissivity

Consider a typical cylindro-cone blackbody for fixed-point calibrations (length L = 50 mm, aperture diameter d = 8 mm (normal case) or aperture diameter d = 2 mm (best case), cone half-angle θ = 30°, wall emissivity ε = 0.85). This results in an emissivity of ε_{BB} = 0.9995 for the cavity in the normal case and ε_{BB} = 0.99997 in the best case. The following values are all standard deviations.

1. Wall emissivity: The wall emissivity ε for graphite is generally between 0.8 and 0.9, depending on the graphite used, and the accepted values for a given graphite have a spread of about ±0.02. However, during machining, the graphite is polished to some extent and develops specularity, so a standard uncertainty of 0.025 is more realistic.
$$\partial \varepsilon_W \approx (1 - \varepsilon_{BB})\, \Delta\varepsilon / (1-\varepsilon) \quad (2)$$

2. Temperature gradients: The front of the cavity and aperture is not fully enclosed by the liquid-solid metal interface, so may be expected to be cooler. Assuming the whole cavity except the base is cooler by ΔT:
$$\partial \varepsilon_T \approx c_2/(\lambda T^2)\, (1-\varepsilon)\, \Delta T \quad (3)$$

(this is a worst case: generally only the aperture is cooler: the table gives results for a linear gradient of 50 mK for normal uncertainty and 25 mK for best uncertainty).

3. Geometrical factors: The cavity dimensions are not perfectly well known. Assume for normal uncertainty ΔL = 1 mm, Δd = 0.25 mm, and $\Delta\theta$ = 2.5° (For best uncertainty the values are half of these numbers).
$$\partial \varepsilon_l \approx (1 - \varepsilon_{BB})\, 2\, \Delta L/L \quad (4)$$
$$\partial \varepsilon_d \approx (1 - \varepsilon_{BB})\, 2\, \Delta d/d \quad (5)$$
$$\partial \varepsilon_\theta \approx (1 - \varepsilon_{BB})\, \cot\theta\, \Delta\theta \quad (6)$$

4. Machining imperfections: During construction about Δt = 0.25 mm of the tip of the conical cavity is slightly rounded (surface locally ⊥ cavity axis), with a consequently lower local effective emissivity. The pyrometer collects radiation from a small region of the base, say t = 2 mm.
$$\partial \varepsilon_{machining} \approx (1-\varepsilon_{BB})\, (\mathrm{cosec}\, \theta - 1)\, (\Delta t/t)^2 \quad (7)$$

Uncertainty budget (Emissivity):

quantity X_2	estimate x_2	standard uncertainty $u(x_2)$		probability distribution	sensitivity coefficient c_2	uncertainty contribution $u_2(y)$			
						at T_{ref}		at 3000 K	
		normal value	best value			normal value	best value	normal value	best value
ε_{BB}	0.9995 / 0.99997								
$\partial\,\varepsilon_w$	0	0.00010	0.000006	normal	$\lambda T^2/c_2$				
$\partial\,\varepsilon_T$	0	0.00004	0.000020	normal	$\lambda T^2/c_2$				
$\partial\,\varepsilon_L$	0	0.00002	0.0	normal	$\lambda T^2/c_2$				
$\partial\,\varepsilon_d$	0	0.00003	0.000003	normal	$\lambda T^2/c_2$				
$\partial\,\varepsilon_\theta$	0	0.00004	0.000001	normal	$\lambda T^2/c_2$				
$\partial\,\varepsilon_{machining}$	0	0.00002	0.000001	normal	$\lambda T^2/c_2$				
$\partial\,\varepsilon_{BB}$	0	0.00012	0.000021	normal	$\lambda T^2/c_2$	10 mK	2 mK	49 mK	9 mK

2.1.1.3 Temperature drop

The loss of radiant energy through the aperture produces a temperature drop at the cavity bottom between the metal surface and the inner cavity wall. According to [9] this temperature drop can be calculated using the following formula:

$$\Delta_b(T) \approx \varepsilon_{tot}\sigma T^4 (d/\kappa)(r/L)^2 \qquad (8)$$

where:
$\Delta_b(T)$ is the temperature drop,
ε_{tot} is the total emissivity of graphite,
σ is the Stefan-Boltzmann constant,
T is the temperature in Kelvin,
d is the thickness of the cavity bottom,
κ is the thermal conductivity of graphite,
r is the aperture radius, and
L is the cavity length.

The largest contribution to the uncertainty in this correction stems from the assumed value for the thermal conductivity and, partially, from the uncertainty in the thickness of the cavity bottom. Since the thermal conductivity of a graphite sample depends on many physical and chemical factors it is very difficult to compare values from different studies, or to predict what the value for a particular specimen is likely to be. The problem is made worse by much of the literature giving very little additional information about the samples; in particular thermal conductivity values are often given without specifying the temperature at which they were measured. Manufacturers' data are not always reliable since a 'typical' value is usually quoted. Actual values can vary between samples of the same batch, as well as between specimens from one sample.

If an accurate value for the thermal conductivity of a sample is required, it is best to have it measured directly. It should be measured along the direction of interest to prevent errors due to anisotropy, as well as at the temperature(s) required. However, for this application, it is probably sufficient to estimate the value from the literature, or from the manufacturer's specifications. Providing the resulting uncertainty can be tolerated, values can also be extrapolated to different temperatures using a typical thermal conductivity / temperature dependence. Details can be found in the very recent study of McEvoy and Machin [10].

In any case, the contribution to the uncertainty budget is limited in extent, typically only a few millikelvin.

Uncertainty budget (Temperature drop):

quantity X_3	estimate x_3	standard uncertainty $u(x_3)$		probability distribution	sensitivity coefficient c_3	uncertainty contribution $u_3(y)$			
						at T_{ref}		at 3000 K	
		normal value	best value			normal value	best value	normal value	best value
$\Delta_b(T)$	10 mK	5 mK	2 mK	rectangular	$(T/T_{ref})^2$	5 mK	2 mK	25 mK	10 mK

2.1.1.4 Plateau identification

The plateau identification is closely related to the shape of the freezing curve. State-of-the-art furnaces give sufficiently long plateaus (see 2.1.1.5) and consequently the identification is of only minor influence on the uncertainty. Typical standard deviations of the recorded readings result in the values given in the table below.

Uncertainty budget (Plateau identification):

quantity X_4	estimate x_4	standard uncertainty $u(x_4)$		probability distribution	sensitivity coefficient c_4	uncertainty contribution $u_4(y)$			
						at T_{ref}		at 3000 K	
		normal value	best value			normal value	best value	normal value	best value
∂ plateau	0	5 mK	1 mK	rectangular	$(T/T_{ref})^2$	5 mK	1 mK	25 mK	5 mK

2.1.1.5 Repeatability

This component includes:

- signal noise of the thermometer
- resolution of the voltmeter
- short-time stability of the detector

Multiple heating zone furnaces and heat-pipe furnaces give sufficient thermal uniformity to reach a repeatability of the freezing curves within typically 10 mK (68.3% confidence level). Typically, melting and freezing plateaus of 30 min to 100 min duration are achieved. This allows the integration time of the radiation thermometer to be made sufficiently long that the repeatability is dominated by the noise of the thermometer (with an adequate effective wavelength). Before the freezing is initiated the furnace is given a homogeneous and stationary temperature distribution e.g. 2 K above the freezing point for at least one hour. The freezing can be initiated either by a sudden reduction in heating power or by introducing a constant cooling rate (e.g. 0.5 K/min) for a limited time period. No significant influence of these two methods has been found on the repeatability of the freezing plateau as long as the cooling rate is not chosen too low, which may then result in an imperfect shape of the interface between the solid and liquid phase leading to a higher curvature of the freezing curves.

Uncertainty budget (Repeatability):

quantity X_5	estimate x_5	standard uncertainty $u(x_5)$		probability distribution	sensitivity coefficient c_5	uncertainty contribution $u_5(y)$			
						at T_{ref}		at 3000 K	
		normal value	best value			normal value	best value	normal value	best value
∂ repeat	0	20 mK	5 mK	normal	$(T/T_{ref})^2$	20 mK	5 mK	101 mK	25 mK

2.1.2 Uncertainty in the spectral responsivity measurements

The overall spectral responsivity of a radiation thermometer depends on the relative spectral response of the detector, the transmission profile of the interference filter and any neutral filters and the transmission of any other optical components (e.g. lenses). The combination of these enables the spectral responsivity and 'effective wavelength' of the instrument to be determined. Since the detector responsivity and the transmis-

sion of the optical components usually vary slowly with wavelength, the dominant component of the effective wavelength is the transmission profile of the interference filter.

Ideally the radiation thermometer should be calibrated as an entity. Interreflections between optical components can be significant and complex and so the signal can be under- or overestimated by separate calibrations of the detector and filter.

The conventional method for deriving the spectral responsivity of a standard radiation thermometer uses a monochromator [11]. In using such a device the following operations are performed:

(a) wavelength calibration of the monochromator.
(b) measurement of the output of the monochromator with a reference detector at each wavelength. (The input spectral curve for the thermometer)
(c) measurement of the signal from the thermometer at each wavelength (The output spectral curve for the thermometer)
(d) calculation of the spectral responsivity as the ratio of the output to the input spectral curves.
(e) Calculation of the effective wavelength for the thermometer (see 2.1.2.7).

Alternatively a tuneable laser source, as described in [12], can be used. In this example the laser output is passed through an optical fibre in an ultrasonic bath to average out the effects of coherence and then an integrating sphere to produce a Lambertian angular variation of the radiance. Both the fibre and the integrating sphere reduce the polarisation. The wavelength of a laser has negligible bandwidth, can be accurately determined, and the signal is also usually higher. All these factors reduce the size of the uncertainties, however this technique is more expensive and usually more time consuming.

2.1.2.1 Wavelength Uncertainty and Bandwidth

The wavelength accuracy of the monochromator can be determined by using emission lines from spectral lamps (eg Ne, Ar, Hg) or laser lines. There are three categories of wavelength error:

- ✓ An offset, which can be removed by subtraction, due to errors in the optical alignment of the gratings and mirrors in the monochromator.
- ✓ A systematic error in the grating drive mechanism resulting in different calibration offsets at different wavelengths. This can be minimised by careful monochromator choice, or by using a mathematical model based on detailed measurement at many wavelengths.
- ✓ A residual uncertainty due to the random effects (such as ambient temperature and humidity) and miscorrection of the previous two (for a good monochromator this is approximately 0.05 nm).

An additional uncertainty is caused by the bandwidth of the monochromator. If this is a significant proportion of the bandwidth of the thermometer's filter, then the spectral responsivity curve will be "averaged out" resulting in broadening of the transmission profile and loss of structure around the peak, as shown in figure 1.

This broadening is most significant at wavelengths and blackbody temperatures where the blackbody spectral radiance curve is rising sharply, since the broadening will give the appearance of shifting some of the centre of the responsivity profile to higher or lower wavelengths where the blackbody has a different radiance. In this example, for an effective wavelength of approximately 648 nm and measuring a blackbody at the gold point, the effective wavelength will increase by 0.03 nm with a 6 nm monochromator bandwidth (equivalent to 0.3 K at 3000 K), or 0.01 nm with a 4 nm monochromator bandwidth (equivalent to 0.1 K at 3000 K), compared to that calculated with a 0.5 nm bandwidth at the same calibration step size of 1 nm.

These effects are far less important with a laser source calibration, since the wavelength can be accurately measured and the bandwidth is negligible, but for radiation thermometry applications this bandwidth effect is not of major significance. The entire radiation thermometer should be calibrated as an entity to account for interreflections. However, if calibrated separately, the uncertainty due to inaccurately determining the spectral response of the detector is far smaller than that due to the filter, since the detector response typically is relatively flat over the spectral region of the filter. Even if the detector response is assumed to be completely flat, the uncertainty in the effective wavelength would be only of the order of 0.02 nm.

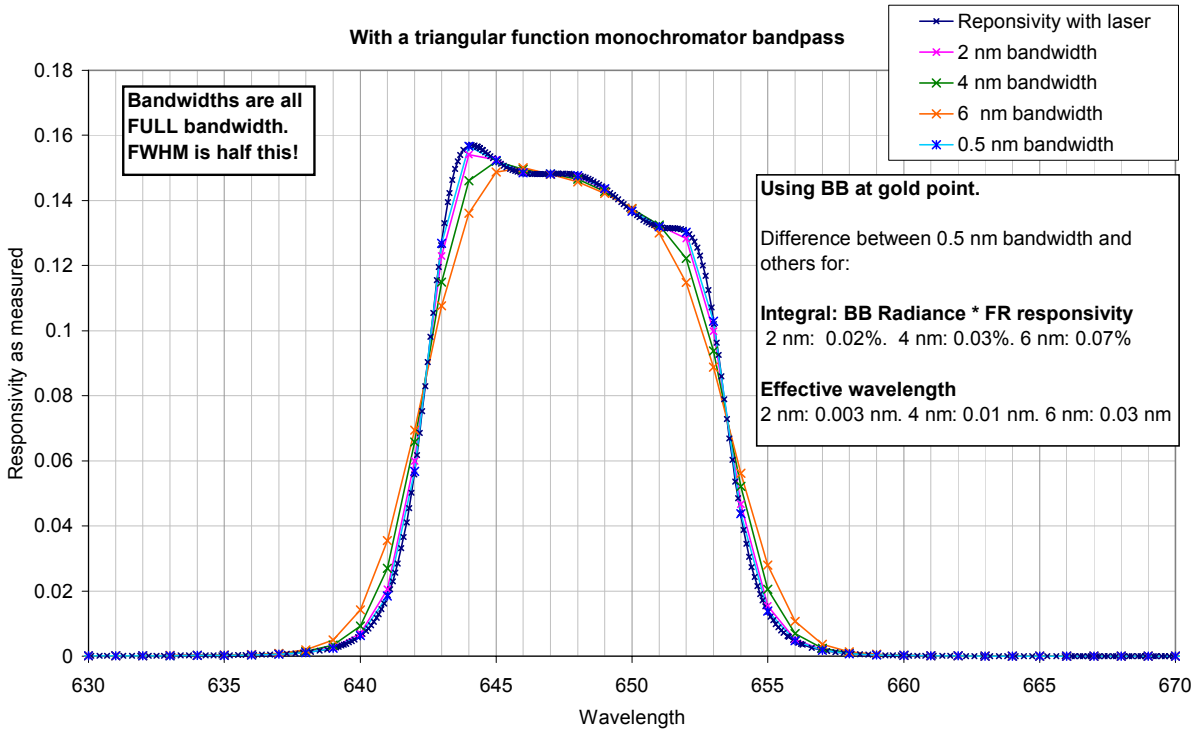

Figure 1: Simulation of result expected if thermometer is calibrated with a monochromator source with a triangular slit function, rather than with a laser. Real laser calibration shown as dark blue line. The lines are only for connecting the symbols. (Note that the term 'bandwidth' in the figure refers to the monochromator not the filter bandwidth).

Uncertainty budget (Wavelength):

quantity X_6	estimate x_6	standard uncertainty $u(x_6)$		probability distribution	sensitivity coefficient c_6	uncertainty contribution $u_6(y)$			
						at T_{ref}		at 3000 K	
		normal value	best value			normal value	best value	normal value	best value
$\partial\lambda^{(1)}$	0	0.08 nm	0.03 nm	rectangular	$\left(\frac{T}{\lambda}\right)\left(\frac{T}{T_{ref}}-1\right)$	0 mK	0 mK	464 mK	166 mK
$\partial\lambda^{(2)}$	0	0.003 nm	0.0006 nm	rectangular	$\left(\frac{T}{\lambda}\right)\left(\frac{T}{T_{ref}}-1\right)$	0 mK	0 mK	17 mK	3 mK

(1) using a monochromator; the uncertainties due to both wavelength and bandwidth (assumed to be 4 nm for the 'normal' case) have been included.
(2) using the laser source calibration technique.

2.1.2.2 *Reference detector*

Typically the reference detector is a solid-state photodiode that has been calibrated against a spectrally flat detector. This can be an absolute detector, such as a cryogenic radiometer, or a relative detector, such as a blackened pyroelectric detector or thermopile. Sometimes these relative detectors are used directly as the reference detector, however better uncertainties can often be achieved with solid-state devices because of their improved signal to noise characteristics. A particularly good solid-state detector is the silicon trap detector, since it has a highly predictable response due to its "quantum flat" nature. The spectral flatness of the response of thermal detectors should be checked experimentally either by reference to an absolute detector or by a direct measurement of reflectance. Assuming it is flat based on published data may lead to errors as its properties can change depending on the surface coating. In addition to the uncertainty in the reference detector primary calibration, there will be uncertainties due to the repeatability (signal to noise), alignment (especially for a non-uniform detector, or one sensitive to tilt), temperature stability and ageing of the reference detector. The 'normal' uncertainties in the table below correspond to the case where a blackened pyroelectric detector is used as the reference detector. As can be seen, the uncertainties are very small. The 'best' uncertainties, achievable by using a trap detector, are even smaller and are therefore assumed to be negligible.

Uncertainty budget (Detector):

quantity X_7	estimate x_7	standard uncertainty $u(x_7)$		probability distribution	sensitivity coefficient c_7	uncertainty contribution $u_7(y)$			
						at T_{ref}		at 3000 K	
		normal value	best value			normal value	best value	normal value	best value
∂ detector	0	0.00018 nm	0 nm	rectangular	$\left(\frac{T}{\lambda}\right)\left(\frac{T}{T_{ref}}-1\right)$	0 mK	0 mK	1 mK	0 mK

2.1.2.3 Scattering and Polarisation

Scattering inside the monochromator can mean that light at different wavelengths is transmitted. This light may be detected by the reference detector, but not by the radiation thermometer. Also, excessive stray light means that, using a single monochromator, the out-of-band blocking of the interference filter can only be determined to generally a few parts in 10^5, whereas use of a double monochromator can reduce this to about one part in 10^7 or better.

Where possible, polarisation of the source and polarisation sensitivity of the thermometer should both be minimised. Blackbody sources have no polarisation, however transfer standard lamps and calibration sources do show some degree of polarisation. The polarisation sensitivity of the detector can be reduced by including as few optical elements as possible, ensuring that those optics are in a stress-free mounting and by illuminating all optical components normally and on axis. The polarisation of calibration sources can be minimised by using an integrating sphere source both with the laser and on the exit slit of the monochromator. Polarisation sensitivity of the thermometer and polarisation of the source can be measured by using a polariser in the beam in both orientations. If a particular pyrometer is found to be sensitive to polarisation, then the uncertainty this introduces should be calculated. In the table below, the uncertainty due to polarisation is assumed to be negligible.

Uncertainty budget (Scattering and polarisation):

quantity X_8	estimate x_8	standard uncertainty $u(x_8)$		probability distribution	sensitivity coefficient c_8	uncertainty contribution $u_8(y)$			
						at T_{ref}		at 3000 K	
		normal value	best value			normal value	best value	normal value	best value
∂ scatter	0	0.0009 nm	0.0006 nm	rectangular	$\left(\frac{T}{\lambda}\right)\left(\frac{T}{T_{ref}}-1\right)$	0 mK	0 mK	5 mK	3 mK

2.1.2.4 Repeatability of Calibration

Noise in the thermometer is a source of uncertainty that can be estimated as a type A uncertainty by repeat measurement (although other sources of uncertainty e.g. reference detector noise and “random” wavelength uncertainties etc, will also be present in any repeat measurement). Higher signals will give a better signal to noise and therefore should be used where possible. A laser-integrating sphere source normally has a higher signal than a monochromator source. By widening the bandwidth, the signal of the monochromator source will be improved, however a compromise must be made, since this will introduce the bandwidth effects described above.

Alignment

Interference filters are sensitive to the angle of incidence of the beam (tilting the filter by 5° reduces the value of the centre wavelength by about 0.6 nm) and some detectors are not perfectly uniform in response. For this reason it is important that the radiation thermometer is calibrated in the same geometry as it will be used. The calibration beam should be uniform and overfill the thermometer with an F-number matching that in use. Any variation will be a source of uncertainty. However, pyrometers tend to be fixed systems and the orientation and alignment of the components are not changed. Therefore, this uncertainty component is assumed to be very small.

Temperature sensitivity

Similarly, radiation thermometers are sensitive to ambient temperature and should be held at a constant temperature for both calibration and measurement. The responsivity of the thermometer varies with ambient temperature due to:

1) a shift in the centre wavelength of the filter and changes in its transmission due to the temperature coefficient of the filter (typically 0.03 nm/°C). Generally, the peak transmission shifts to longer wavelengths with increasing temperature. An uncertainty will arise both due to the measurement of the temperature coefficient and to applying this correction during use. (Variation in repeated measurements of the temperature coefficient of an interference filter using conventional techniques is approximately 0.008nm/°C, giving an estimate for the uncertainty in measuring it. Assuming ambient temperature varies by ± 2°C this leads to a maximum uncertainty in the filter wavelength of 0.010 nm).

2) Changes in the detector response (at longer wavelengths). For example, for a silicon photodiode operating at 900 nm, changes in the output signal with temperature are minimal since the thermometer is operating in the flat portion of the detector response. At shorter wavelengths it has been reported [13] that the signal decreases with increasing ambient temperatures, although modern detectors are less prone to temperature effects [14]. However, major effects occur at wavelengths beyond the peak responsivity where detectors are very sensitive to changes in ambient temperature. This is greatly negated by working at or below the peak response wavelength, well away from the cutoff.

Uncertainty budget (Repeatability):

quantity X_9	estimate x_9	standard uncertainty $u(x_9)$		probability distribution	sensitivity coefficient c_9	uncertainty contribution $u_9(y)$			
						at T_{ref}		at 3000 K	
		normal value	best value			normal value	best value	normal value	best value
∂ align	0	0.0006 nm	0.0006 nm	rectangular	$\left(\frac{T}{\lambda}\right)\left(\frac{T}{T_{ref}}-1\right)$	0 mK	0 mK	3 mK	3 mK
∂ temp	0	0.012 nm	0.0017 nm	rectangular	$\left(\frac{T}{\lambda}\right)\left(\frac{T}{T_{ref}}-1\right)$	0 mK	0 mK	66 mK	10 mK
∂ *signal to noise*	0	0.00028 nm	0.00028 nm	normal	$\left(\frac{T}{\lambda}\right)\left(\frac{T}{T_{ref}}-1\right)$	0 mK	0 mK	2 mK	2 mK
∂ repeat						0 mK	0 mK	66 mK	11 mK

2.1.2.5 Drift

The spectral response characteristics of a radiation thermometer are known to change over time due to ageing of the filter and, to a lesser extent, of the detector. This drift may not be steady over time, and can occasionally show sudden jumps of up to 1% in spectral responsivity. Filter ageing is mainly due to the relaxation of the layers in the interference filter and is difficult to predict, since it is very dependent on the ambient conditions during use and storage. Typically, the centre wavelength of the filter increases by 0.06 nm per year, but changes of up to 0.2 nm per year have been observed. Therefore radiation thermometers should be calibrated regularly and measurements of a blackbody should always be made with more than one radiation thermometer or with a radiation thermometer that has the facility of working at more than one independently characterised wavelength. (Typical uncertainty component due to drifts, assuming re-calibration of the filters once a year, is 0.03 nm to 0.12 nm).

Uncertainty budget (Drift):

quantity X_{10}	estimate x_{10}	standard uncertainty $u(x_{10})$		probability distribution	sensitivity coefficient c_{10}	uncertainty contribution $u_{10}(y)$			
						at T_{ref}		at 3000 K	
		normal value	best value			normal value	best value	normal value	best value
∂ drift	0	0.12 nm	0.03 nm	rectangular	$\left(\frac{T}{\lambda}\right)\left(\frac{T}{T_{ref}}-1\right)$	0 mK	0 mK	663 mK	166 mK

2.1.2.6 Out-of-band transmittance

The spectral response of the radiation thermometer outside the calibrated range should be zero. The quality of a filter is partly determined by its ability to block radiation of all wavelengths outside the central band, and often a blocking filter, pairs of filters, or an additional wideband interference filter should be used to reduce the out-of-band transmittance. Improving the blocking to 1×10^{-7} gives an error of only 0.2 mK at the Ag point [15], but this is difficult to achieve. Usually blocking of $<1 \times 10^{-5}$ is easily achievable.

In practice, out-of-band transmission of the filter at relatively short wavelengths is not a major problem since at these wavelengths the blackbody emits less light and the photon detectors have a lower responsivity. At longer wavelengths, however, the out-of-band transmittance becomes much more significant. Broad and shallow or narrow but strong side peaks, even at wavelengths far away from the main transmission peak, can have a significant effect on the responsivity and hence the mean effective wavelength of the thermometer. For example, an interference filter with a centre wavelength of approximately 660 nm but which has a side peak, giving a transmission of 80 % of the peak above 1150 nm, where the response of a silicon detector is low, can still lead to errors of 3.5 °C in the measurement of the comparably narrow Ag-Au interval.

The out-of-band transmittance must be measured and, if significant, subtracted. This can be done by continuing the calibration with a monochromator at larger wavelength steps into the longer wavelengths. The disadvantage with this is that it may miss narrow features.

Alternatively, measurements can be made in front of the test blackbody using a long-pass filter that cuts on just after the highest calibration wavelength. Ideally the filter cut on should be as sharp as possible, the short wavelengths should be completely blocked (otherwise the out-of-band is overestimated) and the longer wavelength transmission should be near unity (otherwise the out-of-band is underestimated). Variations from this will introduce their own uncertainties, but in this way narrow features will be found.

The following table assumes that the effect of out-of-band transmittance for a particular system has been evaluated and a correction applied. The quoted values represent the uncertainty after the correction has been applied.

Uncertainty budget (Out-of-band transmittance):

quantity X_{11}	estimate x_{11}	standard uncertainty $u(x_{11})$		probability distribution	sensitivity coefficient c_{11}	uncertainty contribution $u_{11}(y)$			
						at T_{ref}		at 3000 K	
		normal value	best value			normal value	best value	normal value	best value
∂ block	0	0.015 nm	0.002 nm	rectangular	$\left(\frac{T}{\lambda}\right)\left(\frac{T}{T_{ref}}-1\right)$	0	0	86 mK	11 mK

2.1.2.7 Integration and Interpolation

The uncertainties discussed in this section are those arising solely from the numerical manipulation of equations involving the spectral responsivity. That is, it is assumed that the measured spectral responsivity has zero uncertainty. Uncertainties in the measured spectral responsivity are dealt with in the sections above. There are two approaches to determining temperature, T, on ITS-90 above the silver point: the integral equation approach and the mean effective wavelength approach. Each gives rise to a different uncertainty contribution.

Integral Equation Approach

The integral equation approach directly solves the equation

$$\frac{S(T)}{S(T_{\mathrm{ref}})}=\frac{\int_0^\infty R(\lambda)L_{\mathrm{b}}(\lambda,T)d\lambda}{\int_0^\infty R(\lambda)L_{\mathrm{b}}(\lambda,T_{\mathrm{ref}})d\lambda}\approx\frac{I(T)}{I(T_{\mathrm{ref}})}, \tag{9}$$

where T_{ref} is the temperature of either the silver, gold, or copper point, and $R(\lambda)$ is the spectral responsivity of the pyrometer. Uncertainty in the calculated temperature arises from differences between the exact values of the integrals in eq. (9) and their numerical approximations, $I(T)$ and $I(T_{\mathrm{ref}})$. The integration error depends upon the spacing of the wavelengths at which $R(\lambda)$ is sampled and the shape of the responsivity curve (but not the centre wavelength or the bandwidth).

The uncertainty in the calculated temperature, u_T, has an upper limit of

$$u_T = \frac{\lambda T^2}{c_2}\left[\left(\frac{u_{I(T_{\text{ref}})}}{I(T_{\text{ref}})}\right)^2 + \left(\frac{u_{I(T)}}{I(T)}\right)^2\right]^{1/2}, \qquad (10)$$

where λ is the centre wavelength of the spectral responsivity. This uncertainty can be made arbitrarily small by increasing the number of points in the integration process. For the product λT^2 in the range 1 m·K^2 to 10 m·K^2, u_T is less than 0.1 mK if at least 30 equally-spaced points are used in the integration for a Gaussian shaped spectral responsivity, and at least 45 points for an interference filter shaped spectral responsivity. For the same λT^2 range, u_T is approximately 1 μK for both spectral shapes if 50 integration points are used. It is assumed that Simpson's rule is used for the integration.

Mean Effective Wavelength Approach

The second approach is to equate the signal ratio of eq. (9) to the right-hand side of eq. (1), with λ equal to the mean effective wavelength, λ_m, which is a function of both T and T_{ref}. (This is discussed in detail in ref. [16] and summarised here.) In practice, the mean effective wavelength is usually determined from the limiting effective wavelength, λ_T, which is calculated from the spectral responsivity and is a function of only a single temperature. Approximations inherent in this process produce an error, $\Delta\lambda_m$, in the value of λ_m, which in turn gives rise to an error in the calculated value of T equal to

$$\Delta T = T\left(\frac{T}{T_{\text{ref}}} - 1\right)\frac{\Delta\lambda_m}{\lambda_m}. \qquad (11)$$

The value of $\Delta\lambda_m$ is a function of the bandwidth, centre wavelength and shape of the spectral responsivity, and of the temperature range over which λ_T is determined. For both Gaussian and interference filter shaped spectral responsivities with a full width at half maximum less than 20 nm, ΔT is less than 1 mK for centre wavelengths from 650 nm to 900 nm and for temperatures up to 3000 °C. It is interesting to note that ΔT increases if exact rather than interpolated values of λ_T are used [16].

Uncertainty budget (Integration and Interpolation):

quantity X_{12}	estimate x_{12}	standard uncertainty $u(x_{12})$		probability distribution	sensitivity coefficient c_{12}	uncertainty contribution $u_{12}(y)$			
						at T_{ref}		at 3000 K	
		normal value	best value			normal value	best value	normal value	Best value
∂T_{int}	0	0.1 mK	0.001 mK	rectangular	1	0 mK	0 mK	0.1 mK	0.001 mK
$\partial \lambda_m$	0	0.014 nm	0.00002 nm	rectangular	$\left(\frac{T}{\lambda}\right)\left(\frac{T}{T_{ref}} - 1\right)$	0 mK	0 mK	83 mK	0.1 mK

2.1.3 Uncertainty in the output signal

2.1.3.1 Size-of-source effect (SSE)

SSE corrections are required in order to render the realisation of the ITS-90 independent of the characteristics of the thermometer actually used. This is also a necessary prerequisite for making possible scale comparisons among different laboratories. Frequently, the main reason for the SSE are aberrations of the image system of the radiation thermometer.

The correction for the SSE applies to both the approaches, i.e., the fixed-point calibration transferred to a lamp or alternatively maintained on the thermometer itself. When pyrometric lamps are used, a lamp whose filament is at the same radiance temperature as a fixed-point blackbody, will give rise to a different thermometer output because of the different contribution from the surroundings. Normally, the contribution from the lamp will be lower than that from the fixed-point blackbody and consequently the corresponding signal will be lower. Thus, when comparing a lamp with a blackbody, in the first instance one will assign to the lamp a current value generally in excess that depends on the SSE characteristics. A good practice is to adjust the current value determined experimentally at the fixed point by an amount corresponding to the SSE.

In the scheme 3 for the ITS-90 realisation, i.e., the fixed-point calibration maintained on the thermometer, SSE corrections are required to normalise the fixed point calibration to a given reference diameter. The

measured fixed-point signal will be corrected by an amount corresponding to the stray radiation. In practice, depending on the actual aperture diameter, on the reference diameter and on the temperature distribution, SSE corrections may be in the sense of both increasing or decreasing the signal.

The SSE correction SSE_{corr} can be expressed in terms of spectral radiance by the following equation:

$$SSE_{corr} = \frac{\Delta L_{\lambda,T_{ref}}}{L_{\lambda,T_{ref}}} = q(SSE) + \partial SSE + \partial L_{distr} + \partial L_{Tstrip} + \partial L_{drift} \qquad (12)$$

where:

$q(SSE)$: "SSE correction factor" to be used for correcting the spectral radiance $L_{\lambda,Tref}$
∂SSE: correction on basis of the deviation of the SSE from the measured curve
∂L_{distr}: correction due to the radial temperature distribution of the fixed-point cavity
∂L_{Tstrip}: correction due to the temperature distribution along the lamp filament
∂L_{drift}: correction due to the drift of the SSE characteristics

SSE correction factor ($q(SSE)$): to be applied to the measured spectral radiance $L_{\lambda,Tref}$; $q(SSE)$ is calculated making use of the SSE distribution curve and the temperature distribution of the sources, i.e., the fixed-point blackbody cavity and, in case it is used, the tungsten strip lamp.

SSE measurement (∂SSE): uncertainty component related to the measurement of the SSE characteristics of the standard thermometer. Major sub-components derive from:

- radiance uniformity of the source
- radiance stability of the source
- spectral distribution of the source
- inter-reflections between the source and the radiation thermometer
- non-blackness of the of the black spot (applying only to the indirect method)
- dimension of the aperture diaphragms and, in case of indirect method, of the black spots, both circular and strip spots
- aiming and orientation
- signals measurement
- repeatability
- polynomial fit
- reproducibility

Estimates for the uncertainty in SSE measurement are generally low, e.g., some units in 10^{-4} and 10^{-5} in terms of spectral radiance for normal and best realisations, respectively. However, it must be evidenced that recent investigations [17] suggest that an underestimation of some uncertainty components related to the SSE measurements could occur. The results of the international project TRIRAT ("Traceability in Infrared Radiation Thermometry") [18] evidenced possible additional uncertainties originating from the not completely accounted for "out-of-focus stray radiation". In addition, the out-of-band radiation caused by imperfect interference filters may enhance the SSE.

On the other hand, it must also be stressed that precision radiation thermometers showing low SSE, e.g., from 1 $x10^{-3}$ to $2x10^{-3}$, and normally used as standard instruments for the realisation of the ITS-90, are not affected very much by these additional uncertainty components. In [19], an agreement of $7x10^{-5}$, corresponding to 6 mK at the Au point at a wavelength of 650 nm, was found by measuring the SSE of a standard radiation thermometer with two different methods. Typical values at the fixed-points, i.e., Ag, Au or Cu, are ranging from a few millikelvin to 0.05 °C [20].

Radial temperature distribution of the fixed-point cavity (∂L_{distr}): The experimental determination of the temperature distribution of the surroundings of the cavity aperture, is necessary to calculate the actual "SSE correction factor" q. Most laboratories perform scans in horizontal direction (some laboratories in vertical direction, too) by using the standard thermometer itself or, in case higher sensitivity is required to detect lower temperatures, a longer wavelength thermometer. Uncertainty estimates for determining the complete temperature distributions are claimed to be 1 K in case of best realisations [21].

Some laboratories experimentally derive the correction coefficient q directly with an "in situ" measurement by using a dummy blackbody crucible [22, 24] or a specially designed cooled simulator [25]. The coefficient q is derived as the ratio of stray radiation signal obtained with the simulator to the fixed-point signal. An "effective

radiating diameter" is defined as the "virtual diameter" from which the detected stray radiation originates. Uncertainty in the "effective radiating diameter" is estimated to be about 1 mm for the best ITS-90 realisations.

Temperature distribution of lamp filament (∂L_{Tstrip}): this component only applies to the realisation schemes 1 and 2. Generally, the temperature is assumed to be uniform. Very few laboratories scan the filament in both horizontal and vertical directions. Due to the limited radiating area of the filament, e.g., 3% with respect to a blackbody cavity 50 mm in diameter, this uncertainty component will have a limited effect on the combined uncertainty.

Drift of the SSE characteristics (∂L_{drift}): There is no evidence of significant variations of the SSE characteristics with time. A proper cleaning of the objective should be sufficient to keep the uncertainty within $1x10^{-5}$ and $5x10^{-5}$ in the best and normal case, respectively.

Uncertainty budget (SSE correction SSE_{corr}):

quantity X_{13}	estimate x_{13}	standard uncertainty $u(x_{13})$		probability distribution	sensitivity coefficient c_{13}	uncertainty contribution $u_{13}(y)$			
						at T_{ref}		at 3000 K	
		normal value	best value			normal value	best value	normal value	best value
$q(SSE)$	$1x10^{-3}$(^)								
∂SSE	0	$2x10^{-4}$	$2x10^{-5}$	rectangular	$\lambda T^2/c_2$	16.2 mK	1.6 mK	81.3 mK	8.1 mK
∂L_{distr}	0	$5x10^{-4}$ (#)	$2x10^{-5}$ (#)	rectangular	$\lambda T^2/c_2$ (*)	40.4 mK	1.6 mK	203.3 mK	8.1 mK
∂L_{Tstrip}	0	$1x10^{-5}$	$1x10^{-5}$	rectangular	$\lambda T^2/c_2$	0.8 mK	0.8 mK	4.1 mK	4.1 mK
∂L_{drift}	0	$5x10^{-5}$	$1x10^{-5}$	rectangular	$\lambda T^2/c_2$	4.0 mK	0.8 mK	20.3 mK	4.1 mK
SSE_{corr}	$1x10^{-3}$(^)					44 mK	3 mK	220 mK	13 mK

(^): the value q=$1x10^{-3}$ does not refer to any real case, also it may represent a realistic condition. Standard radiation thermometers giving rise to the reported value when used in conjunction with fixed point furnaces with radiating diameter of (30-40) mm, are used by a large number of laboratories

(#): derived from values of 10 K and 5 mm for the normal uncertainty in the temperature distribution measurement and for the effective diameter in case of "in situ" determination of the *q(SSE)* coefficient, respectively; corresponding best uncertainties : 1 K and 1 mm, respectively.

(*): the sensitivity coefficient is strictly related to the furnace actually used (dimension of the radiating area) and to the SSE characteristics of the thermometer. Values for the uncertainty contribution of $5x10^{-4}$ and $2x10^{-5}$ seem to be adequate for normal and best value, respectively.

2.1.3.2 Non-linearity

Non-linearity is caused by the non-ideal performance of the detector, electronics, or both. The output signal is a function of the flux incident upon the entrance pupil. We assume this function, which describes the radiation thermometer response to the dimensions of radiant flux (spectral, spatial, angular, temporal, instrument temperature, polarization, environmental conditions, and linearity) can be factored into independent functions that can be characterized in separate experiments. Under this assumption the non-linearity function is the same for all flux attributes.

The non-linearity correction factor, C_L, defined in terms of the measured signal, is determined experimentally using various methods.[1] Generally, it is measured using one of the following techniques: the "superposition method" and the "dual aperture method". With the first method, two radiation sources (generally tungsten strip lamps) and a beam splitter are used to produce successive doublings of the radiant flux at the photodetector. With the second method, a single radiation source is used and flux doublings are produced by a dual aperture device located between the source and the thermometer.

The results are used to correct the output signals during subsequent measurements of blackbodies or ribbon filament lamps:

$$S = S_u \, C_L(S_u) \tag{13}$$

[1] It is also possible to design the scale realization so that the effects of system non-linearity are automatically accounted for; in this case, a separate correction is not required.

where S_u is the (uncorrected) measured signal and S is the corrected signal. The exact form for C_L varies, depending on how the effect is modelled. Some researchers cast the problem in terms of the residual error, equal to $1 - C_L$.

Potential Components for the Uncertainty of the Non-linearity Correction

1. The representative model for the function $C_L(S_u)$ is uncertain (Type B). Model uncertainties typically are expressed in terms of the standard deviation of the fit or the standard uncertainty of the fitted parameters of the model. There may be additional uncertainty associated with the density of the measurements, extrapolation, or interpolation.
2. The veracity of the "separate functions" approximation (Type B). Because it is time consuming and difficult to perform detailed experiments that would determine dependence of the non-linearity with the temperature, spectral, spatial, temporal, or other dimensions, it is difficult to assess this uncertainty component. The best approach is to duplicate the conditions of measurement in the linearity characterization and the radiation temperature experiments.
3. Systematic effects in the methods used to determine the non-linearity (Type B). Common methods to determine non-linearity include flux addition, beam attenuation, and blackbody source temperature. Each technique is subject to particular issues that must be addressed to eliminate potential sources of systematic error; common examples are interreflections, dynamic range (gain ratios), sensor heating, or spectral out-of-band effects.

Note 1: Signal-to-noise limits, at some level, the determination of the non-linearity, especially at low flux levels. However, the same signal-to-noise will be present at these flux levels during the actual experiment, so this component should not be counted in the non-linearity budget.
Note 2: Some tests have demonstrated that with some thermometers the non-linearity may depend on the aperture of the radiation beam, so, whichever method is used, one must ensure that the non-linearity device is not restricting the effective aperture of the thermometer.

According to ITS-90 in the Wien approximation for monochromatic flux

$$T = \frac{1}{\frac{1}{T_X} - \frac{\lambda}{c_2}\ln(r)}, \text{ with } r = \frac{S(T)}{S(T_X)}. \tag{14}$$

where X refers to the reference temperature (copper, gold, or silver freezing points), the signals are corrected for non-linearity, and T is the radiance temperature (dropping the usual "90" subscript for simplicity). In some cases, the method of non-linearity determination combined with method of ITS-90 scale realization casts the problem in terms of an uncertain ratio, not the signals:

$$u_1(T) = \frac{\lambda}{c_2} T^2 \frac{u(r_L)}{r}. \tag{15}$$

Where the subscript on $u(T)$ is an uncertainty component designator, and $u(r_L)$ is the standard uncertainty in the signal ratio arising from the non-linearity correction. In the brightness doubling method (scheme 1), $r = 2$, and the effect is cumulative and correlated as the temperature increases [22]. The number of intervals N is

$$N = \frac{c_2}{\lambda \ln(2)}\left|\frac{1}{T_X} - \frac{1}{T}\right|, \text{ so } u_1(T) = \frac{\lambda}{c_2} T^2 N \frac{u(r_L)}{r}. \tag{16}$$

In the following table for 3000 K a value of $N = 13.2$ has been used.

An alternative description is in terms of the independent signals [23], with C_L determined over the full range of values. Then

$$u_2(T) = \frac{\lambda}{c_2} T^2 \frac{u(S(T)_L)}{S(T)} \text{ and } u_3(T) = \frac{\lambda}{c_2} T^2 \frac{u(S(T_X)_L)}{S(T_X)}, \tag{17}$$

where $u(S(T)_L)$ and $u(S(T_X)_L)$ are the standard uncertainties in the signal for temperatures T and T_X, respectively, arising from the non-linearity correction. This description is more suited to scheme 2 and scheme 3, which differ primarily in the frequency and temporal interval of the fixed-point calibration of the radiation thermometer. Finally, from eq. (13), the relative standard uncertainty in the signal or the ratio of the signal is equal to the relative standard uncertainty of the correction factors C_L.

Uncertainty budget for non-linearity in terms of signal ratios:

quantity X_{14}	estimate x_{14}	standard uncertainty $u(x_{14})$		probability distribution	sensitivity coefficient c_{14}	uncertainty contribution $u_{14}(y)$			
						at T_{ref}		at 3000 K	
		normal value	best value			normal value	best value	normal value	best value
$C_L(r)$	1	0.0003	0.00005	normal	$\frac{\lambda}{c_2} T^2 N$	0	0	1610 mK	268 mK

2.1.3.3 Drift

This component applies only to scheme 3 and results from the combination of the electronic drift of the amplifier and the drift in the detector output and can be separated into zero offset drift and output drift. A realistic estimation of these components may be done only through prolonged studies of the behaviour of the output signal.

Zero offset

The zero offset can be measured by putting a light-tight cap on the objective lens. The measurement should be made after sufficient warming-up time. Usually the zero offsets of different gain ranges change in the same way. Often the zero offset is influenced by the temperature of the detector. When the radiation thermometer receives radiation from a source then the detector temperature increases and the zero offset changes. There is almost a linear correlation between the zero offset and the detector temperature with a typical relative coefficient of –0.001 K^{-1}.

The zero offset can be measured before and after the fixed-point measurement. For example, at NMIJ the zero offset change in the first twenty minutes of a fixed-point measurement corresponds to 0.2 K at the copper point. Because a linear interpolation is made for the zero offset, the uncertainty caused by the zero offset change in the copper point calibration is 0.02 K. Usually three measurements of the copper freezing point agree with each other within 0.02 K. For a LP3 type radiation thermometer the zero offset is stable within $1x10^{-4}$ for one day.

Output drift

The long term stability of a commercial radiation thermometer (Topcon 181) is shown in Figure 2. The outputs at the copper and silver points were measured repeatedly. The output changes within 1.5% in four years. On the other hand the ratio between the copper point and the silver point changed less than 0.2% in the same period. This means that the wavelength did not change but the gain. The gain has the tendency to increase. The decrease by 1 % from the end of 1999 to March of 2000 was caused by contamination of the objective lens and disappeared after cleaning. If the radiation thermometer is calibrated within either six months or half a month, then the change due to the long term drift would be 0.2 % or 0.015 %, respectively.

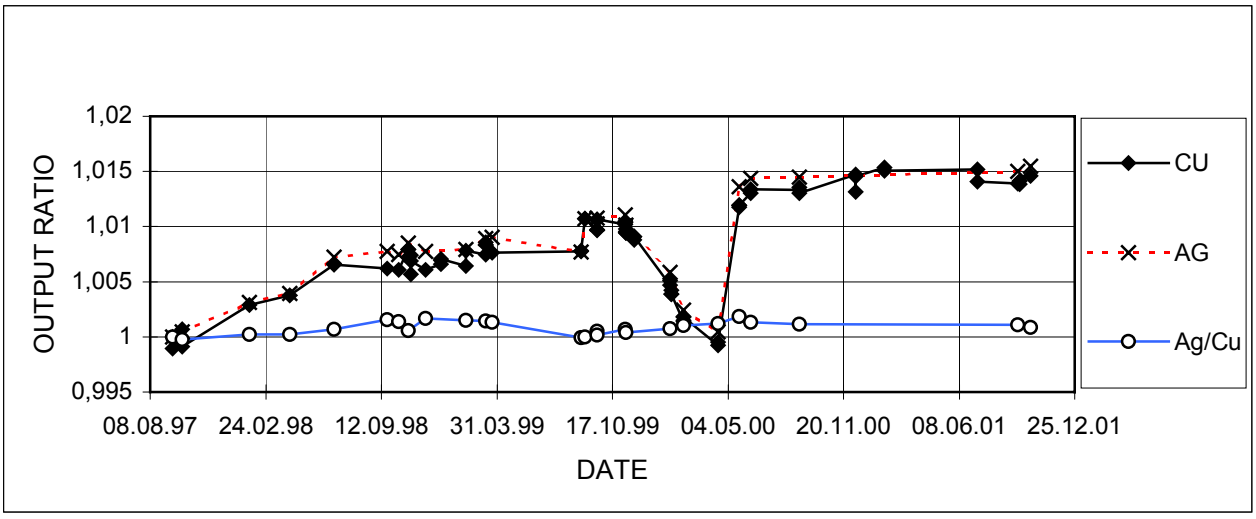

Figure 2: Output drift of a commercial radiation thermometer (Topcon 181)

Uncertainty budget (Drift):

quantity X_{15}	estimate x_{15}	standard uncertainty $u(x_{15})$		probability distribution	sensitivity coefficient c_{15}	uncertainty contribution $u_{15}(y)$			
						at T_{ref}		at 3000 K	
		normal value	best value			normal value	best value	normal value	best value
q(Zero drift)	$1x10^{-3}$	$1x10^{-3}$	$5x10^{-5}$	rectangular	$\lambda T^2/c_2$	80.8 mK	3.2 mK	406.6 mK	20.3 mK
q(Output drift)	$1x10^{-3}$	$2x10^{-3}$	$1x10^{-4}$	rectangular	$\lambda T^2/c_2$	161.6 mK	8.1 mK	813 mK	40.7 mK
∂ Drift	0					181 mK	9 mK	909 mK	45 mK

2.1.3.4 Ambient conditions

This refers to the dependence of the output signal with ambient temperature and relative humidity and applies to scheme 3. Relative humidity does not affect the output signal much for a 0.65 µm radiation thermometer. If the humidity is very high, it is not good for the filter and for the electric circuit. The ambient temperature affects more on the output signal than the humidity. The ambient temperature dependence of seven commercial radiation thermometers (Topcon 181) were determined at NMIJ my measuring a fixed point at different ambient temperatures. All the coefficients lay between –0.05 to +0.05 %/K with an average of the absolute coefficients of 0.026 %/K. Even if the room temperature was constant the detector temperature would change through irradiation due to the target. The amount of the change of the detector temperature is about 1 °C. If this effect is not corrected 0.026 % error would occur in the fixed point measurement. If corrected the error would be 0.005%. The ambient effect is small for a radiation thermometer of the LP3 type because the detector temperature is kept constant at 28 °C. When the ambient temperature was changed from 18 °C to 28 °C then the detector temperature changed from 28 °C to 29.5 °C and the output signal increased by 0.045 %. If the temperature range was from 21 °C to 25 °C, the change in output would be negligible.

To discuss the ambient dependence more in detail, this change was due to the change of the silicon photodiode detector, the filter transmittance and wavelength, electronics circuit and the voltmeter. Therefore if the effect is caused by the filter change, the ambient dependence might be different at other temperature.

Uncertainty budget (Ambient condition):

quantity X_{16}	estimate x_{16}	standard uncertainty $u(x_{16})$		probability distribution	sensitivity coefficient c_{16}	uncertainty contribution $u_{16}(y)$			
						at T_{ref}		at 3000 K	
		normal value	best value			normal value	best value	normal value	best value
q(Ambient)	0	$3x10^{-4}$	$2x10^{-5}$	rectangular	$\lambda T^2/c_2$	24 mK	2 mK	122 mK	8 mK

2.1.3.5 Gain ratios

To cover the temperature range from the Ag point to the highest temperatures, i.e., 2000 °C or more, generally different amplification gains are used. If scheme 2 or scheme 3 are adopted, the knowledge of the gain ratios is required. The relative uncertainty originates from the uncertainty in the measurement of gain ratios and in possible temporal drifts.

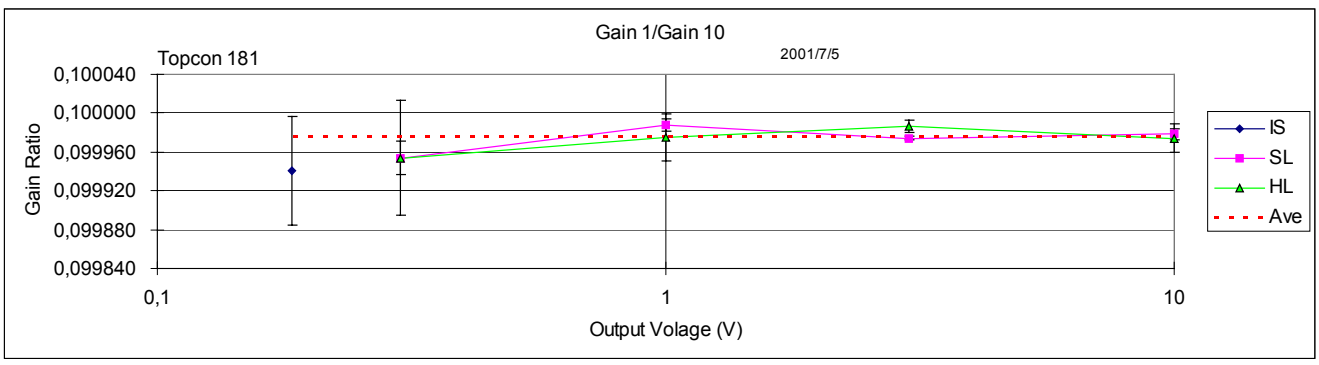

Figure 3: Gain ratio of Topcon 181 between Gain 10 and Gain 1 at various output levels

Figure 3 shows the gain ratio of a radiation thermometer of Topcon 181 type between Gain 10 and Gain 1 at various output levels. An integrating sphere (IS), a standard lamp (SL) and a halogen lamp (HL) were used as radiation sources. The measured gain ratio Gain 1/Gain 10 lies within 0.09998 ±0.00001 for the output voltage from 1 V to 10 V and agrees with those for less than 1 V within the standard deviation. This data shows that the gain ratio does not depend on the output level. This is checking the effect of the linearity and the zero offset. The latter affects more on the gain ratio at the lower output level. In this case the gain ratio was determined as good as 0.01 %.

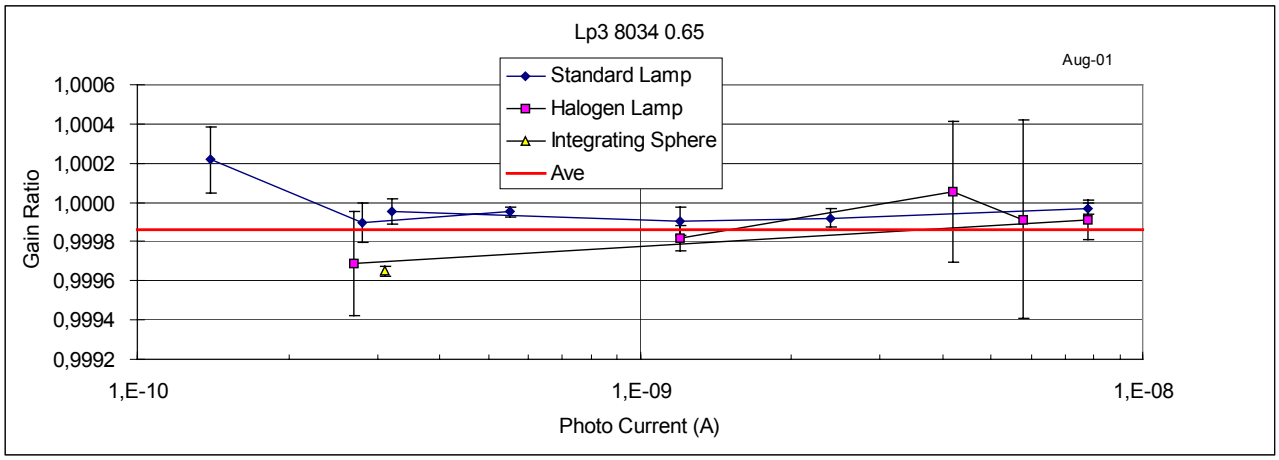

Figure 4: Gain ratio of the LP3

Figure 4 shows the gain ratio of a radiation thermometer of LP3 type between range 1 and 2. The nominal value is 1 and the ratio was determined as 0.9999±0.0001. The IS data has very small standard deviation but differs from the average by 0.0002 which is more than twice the standard deviation.

Uncertainty budget (Gain ratio):

quantity X_{17}	estimate x_{17}	standard uncertainty $u(x_{17})$		probability distribution	sensitivity coefficient c_{17}	uncertainty contribution $u_{17}(y)$			
						at T_{ref}		at 3000 K	
		normal value	best value			normal value	best value	normal value	best value
∂ Gain	0	5×10^{-4}	1×10^{-4}	rectangular	$\lambda T^2/c_2$	40 mK	8 mK	203 mK	41 mK

2.1.3.6 Repeatability

This component includes:

- *signal noise of the thermometer*
- *short term stability of the detector*
- *resolution of the voltmeter*

The signal noise of the thermometer may be significant at the lowest temperatures, i.e., below 1000 °C, as at 650 nm the responsivity of the silicon detector is low. The other two components are not particularly important. The signal noise level has been estimated to be about 0.002% of the output at the copper point. This value is also an estimation of the short term stability of the detector. Modern digital voltmeters have a resolution of 10 nV which corresponds to less than 0.0001% of the output at the copper point.

Uncertainty budget (Repeatability):

quantity X_{18}	estimate x_{18}	standard uncertainty $u(x_{18})$		probability distribution	sensitivity coefficient c_{18}	uncertainty contribution $u_{18}(y)$			
						at T_{ref}		at 3000 K	
		normal value	best value			normal value	best value	normal value	best value
q (Signal Noise)	0	$1x10^{-4}$	$2x10^{-5}$	rectangular	$\lambda T^2/c_2$	8.1 mK	1.6 mK	40.7 mK	8.1 mK
q (Short term stability)	0	$1x10^{-4}$	$2x10^{-5}$	rectangular	$\lambda T^2/c_2$	8.1 mK	1.6 mK	40.7 mK	8.1 mK
q (DVM)	0	$1x10^{-5}$	$1x10^{-6}$	rectangular	$\lambda T^2/c_2$	0.8 mK	0.1 mK	4.1 mK	0.4 mK
∂ Repeat-ability						11 mK	2 mK	58 mK	11 mK

2.1.4 Uncertainty in the lamp measurements

These uncertainty components apply only to scheme 1 and scheme 2. For scheme 1, the use of vacuum lamps (maximum temperature: 1700 °C) and gas-filled lamps give rise to different uncertainty estimations. Accordingly, in the following uncertainty budgets, the values at $T=T_{ref}$ refer to the use of vacuum lamps and the values at T = 2500 K refer to the use of gas-filled lamps. Usually the width of the tungsten strips are between 1.5 mm and 3 mm.

2.1.4.1 Current

The measurement of the lamp current is affected by:

- *uncertainty in the calibration of the voltmeter*
- *uncertainty in the calibration of the standard resistor*
- *presence of a ripple component superimposed on the lamp current*
- *random uncertainty due to resolution of the voltmeter and to the short-term stability of the power supply and the lamp*

Uncertainty budget (Current):

quantity X_{19}	estimate x_{19}	standard uncertainty $u(x_{19})$		probability distribution	sensitivity coefficient c_{19}	uncertainty contribution $u_{19}(y)$			
						at T_{ref}		at 2500 K	
		normal value	best value			normal value	best value	normal value	best value
∂ DVM	0	$1x10^{-5}$	$0.5x10^{-5}$	normal	see below				
∂ resistor	0	$1x10^{-5}$	$0.5x10^{-5}$	normal	see below				
∂ ripple	0	$1x10^{-5}$	$0.5x10^{-5}$	normal	see below				
∂ random	0	$0.5x10^{-5}$	$0.5x10^{-5}$	normal	see below				
∂ current		$1.8x10^{-5}$	$1.0x10^{-5}$			12 mK	7 mK	24 mK	13 mK

Calculation of sensitivity coefficient c_{19} from lamp current i and characteristic of lamp dT/di :

temperature T K	lamp current i A	dT/di K/A	sensitivity coefficient c_{19} K
900	3.7	331	1225
1100	4.6	170	782
1300	6.1	111	677
1500	8.1	87	705
1700	10.6	77	816
1900	13.3	71	944
2100	16.0 *	78	1248
2300	17.3 *	75	1298
2500	18.6 *	72	1339

*above 1900 K gas-filled lamp

It may be more convenient to use the following approximation for the sensitivity coefficient c_{19} :

$$c_{19} = 3.8\text{x}10^{3} - 8\text{x}10^{6} / T + 5.1\text{x}10^{9} / T^{2} \qquad (18)$$

This fits the numbers in the table above to better than 8%.

2.1.4.2 Drift, stability

In principle, this component does not apply to the realisation of the scale, but only to its dissemination. In practice, some drifts may occur during the calibration, particularly with gas-filled lamps in scheme 1. When the calibration is transferred from the vacuum to the gas-filled lamp an additional uncertainty is introduced.

Uncertainty budget (Drift):

quantity X_{20}	estimate x_{20}	standard uncertainty $u(x_{20})$		probability distribution	sensitivity coefficient c_{20}	uncertainty contribution $u_{20}(y)$			
						at T_{ref}		at 2500 K(*)	
		normal value	best value			normal value	best value	normal value	best value
∂ *drift*	0	50 mK	20 mK	rectangular	1	50 mK	20 mK	1050 mK	350 mK

(*) with gas filled lamps

A different uncertainty component $u(x_{20})$ may be introduced for the realisation according to scheme 2. It accounts for the drift of the lamp at the reference point and may be estimated as 5 mK and 20 mK for "best value" and "normal value", respectively.

2.1.4.3 Base and ambient temperature

Uncertainties may derive from:

- ✓ changes in ambient temperature
- ✓ measurement of the base temperature
- ✓ knowledge of the coefficient $\partial T_{\lambda}/\partial T_{base}$

Typical values of $\partial T_{\lambda}/\partial T_{base}$ range from 0.04 at the Ag point to 0.01 at 1100 °C (for higher temperatures the coefficient tends to zero). The temperature stability of the base is 0.2 K and 0.1 K, for the cases normal and best, respectively. In principle, this component may be more critical with scheme 2, as the lamp is always kept at the fixed-point and used as a reference to derive the other temperatures.

Uncertainty budget (Base and ambient temperature):

quantity X_{21}	estimate x_{21}	standard uncertainty $u(x_{21})$		probability distribution	sensitivity coefficient c_{21}	uncertainty contribution $u_{21}(y)$			
						at T_{ref}		at 2500 K	
		normal value	best value			normal value	best value	normal value	best value
∂ *ambient*	0	9 mK	1.7 mK	normal	1	9 mK	1.7 mK	0 mK	0 mK
∂ *base*	0	2 mK	1 mK	normal	1	2 mK	1 mK	0 mK	0 mK
∂ temp-erature						9 mK	2 mK	0 mK	0 mK

2.1.4.4 Positioning

An uncertainty may be introduced if, during the realisation of the scale, the lamps are removed and repositioned. If they are kept in a fixed position this uncertainty component should be zero.

Uncertainty budget (Positioning):

quantity X_{22}	estimate x_{22}	standard uncertainty $u(x_{22})$		probability distribution	sensitivity coefficient c_{22}	uncertainty contribution $u_{22}(y)$			
						at T_{ref}		at 2500 K	
		normal value	best value			normal value	best value	normal value	best value
∂ *position*	0	0.001	0.0002	normal	$\lambda T^2/c_2$	81 mK	16 mK	283 mK	56 mK

2.1.4.5 Polynomial fit

This applies only to scheme 1 and potentially may be the source of one of the most significant contributions to the final uncertainty. (This could be one reason in favour of the adoption of the scheme 2).

Uncertainty budget (Polynomial fit):

quantity X_{23}	estimate x_{23}	standard uncertainty $u(x_{23})$		probability distribution	sensitivity coefficient c_{23}	uncertainty contribution $u_{23}(y)$			
						at T_{ref}		at 2500 K(*)	
		normal value	best value			normal value	best value	normal value	best value
∂ *fit*	0	50 mK	10 mK	normal	1	50 mK	10 mK	100 mK	30 mK

(*) with gas filled lamps

2.2 Uncertainty budget for scales comparison

In practice, a comparison may be intended as a dissemination of the scale, because every participant laboratory has to transfer its scale on the transfer standard used for the comparison. Of course, this may be accomplished in different ways, accordingly to the approach each laboratory followed in the realisation of the scale.
The resulting uncertainty budget must account for the components related to :

- ✓ dissemination of the scale
- ✓ transfer standard
- ✓ normalisation to reference conditions

Note: the analysis will be restricted to the range from 962 °C to 1700 °C, i.e., that of the CCT-K5.

2.2.1 Uncertainty in the dissemination

The main difference with respect to the realisation of the scale concerns the influence of the drift of the lamps. It applies to both scheme 1 and 2. In scheme 2, the lamp is used only at a fixed temperature, i.e., Ag, Au or Cu temperatures and one can account for the drift, provided that the drift rate is known. More critical may be the case of scheme 1, as the lamps are also used at higher temperatures (typical drift rate at 1700 °C for vacuum lamps: 0.3 K/100 h).

2.2.1.1 Cleaning of the windows

The effect of the cleaning of the window in the measurement of the radiance ratios was investigated in [26]. An uncertainty contribution of about 0.1 % in terms of spectral radiance may be estimated.

2.2.2 Uncertainty in the transfer standard

In a comparison at the highest level, as is the case of a key comparison, tungsten strip lamps are still used as transfer standards. The following uncertainty components apply whichever scheme has been adopted in the realisation of the scale.

2.2.2.1 Drift of the transfer standard

This component is related to the burning time of the lamps (in the CCT-K5, a maximum of 30 hours was recommended). On the other hand, as the lamps are used at different temperatures, is not possible to completely account for the drift, as the drift rate is not known at all temperatures. Consequently, considerable uncertainties may originate.

2.2.2.2 Positioning of the transfer standard

Certainly one of the most important sources of uncertainty. Large uncertainties may derive from an insufficient investigation of the system “thermometer-lamp”, as angular distribution of radiance with a peak may occur, due to inter-reflection inside the lamps. Investigations proved that the effect is not a constant but depends on the thermometer actually used. The positioning of the lamp outside the inter-reflection peak is essential to mimimize this uncertainty component.

As the tungsten strip expands with temperature the radiation thermometer is repositioned with respect to the notch for each current setting. Depending on the measured spatial temperature gradients over the strip a significant uncertainty contribution can arise.

Certainly, this component is one of the critical points, as also demonstrated by the large spread of estimated values during the CCT-K5, i.e., from 4 mK up to 0.2 °C.

2.2.3 Uncertainty in the normalisation to reference conditions

In a comparison, to obtain comparable results, corrections should be applied to some influence parameters. In the case of the CCT-K5 [27] the latter were:

- ✓ effective wavelength
- ✓ base temperature of the lamp
- ✓ nominal values of current

2.2.3.1 Effective wavelength

The effective wavelengths of the laboratories participating in the CCT-K5 ranged from 649 nm to 665 nm. The protocol of the comparison required the radiance temperatures T_λ to be referred at λ_r=650 nm, the coefficient $\partial T_\lambda/\partial_\lambda$ ranging from –0.111 °C/nm at 962 °C to –0.307 °C/nm at 1700 °C. Corrections up to more than 4.5 °C were applied by some laboratories. As there was an uncertainty of 10 % of the value of $\partial T_\lambda/\partial_\lambda$, additional uncertainties of several tenths of a degree had to be included. It is worth noting that these uncertainties are part of the uncertainty budget but are not an indication of the skillfulness of the laboratory, as they are simply consequence of a choice for the value of λ_r.

2.2.3.2 Base and ambient temperature

As for the component in 2.2.3.1, uncertainties may derive from:

- ✓ changes in ambient temperature
- ✓ measurement of the base temperature
- ✓ knowledge of the coefficient $\partial T_\lambda/\partial T_{base}$

The uncertainty in the knowledge of $\partial T_\lambda/\partial T_{base}$, 10% of its value in the case of the CCT-K5 [26], requires that the base temperature of the lamps are maintained as close as possible to the nominal temperature. In any case, this component is not a critical one and can easily be maintained within some millikelvin.

2.2.3.3 Current

Generally, in a comparison the results must be referred to some nominal currents. The conversion from the actual currents to the nominal ones may be done by using the coefficient $\partial T_\lambda/\partial I$, to be derived from the polynomial fitting of the measurement data. As in the previous case of the correction for the base temperature, it is possible to reduce the uncertainty by making the actual currents as close as possible to the nominal ones. In the CCT-K5 , uncertainties ranging from 1 mK up to about 0.1 K, regardless of the current value, were claimed by the different laboratories.

The following Table B presents the additional components related to a comparison exercise.

Table B Additional uncertainty components for a comparison exercise

no i	quantity X_i	estimate x_i	standard uncertainty $u(x_i)$		probability distribution	sensitivity coefficient c_i	uncertainty contribution $u_i(y)$			
							at *Tref*		at 1973 K	
			normal value	best value			normal value	best value	normal value	best value
	Dissemination									
24	*∂ drift reference*	0	0.05 K	0.01 K	rectangular	$(T/T_{ref})^2$	0.05 K	0.01 K	0.10 K	0.02 K
25	*∂ window*	0	0.0015	0.001	normal	$\lambda T^2/c_2$	0.12 K	0.08 K	0.26 K	0.18 K
	Transfer standard									
26	*∂ drift transfer*	0	0.05 K	0.01 K	rectangular	1	0.05 K	0.01 K	0.05 K	0.01 K
27	*∂ positioning*	0	0.001	0.0002	normal	$\lambda T^2/c_2$	0.08 K	0.02 K	0.18 K	0.04 K
28	*∂ window*	0	0.0015	0.001	normal	$\lambda T^2/c_2$	0.12 K	0.08 K	0.26 K	0.18 K
	Normalisation									
29	*Δ wavelength*	5 nm	0.1		normal	$dT_\lambda/d\lambda$ (*)	0.1 K		0.15 K	
30	*Δ temperature*	1 K	10 mK	1 mK	normal	1	10 mK	1 mK	10 mK	1 mK
31	*Δ current*	10 mA	10 mK	1 mK	normal	1	10 mK	1 mK	10 mK	1 mK

(*): variation of spectral radiance temperature with wavelength

3. Equation models for the calculation of the uncertainty

According to the *Guide to the Expression of Uncertainty in Measurement* [28] the combined standard uncertainty $u_c(y)$ is derived as the positive square root of the combined variance $u_c^2(y)$ obtained from

$$u_c^2(y) = \sum_{i=1}^{N}\left(\frac{\partial f}{\partial x_i}\right)^2 u^2(x_i) \qquad (19)$$

where $u(x_i)$ is a standard uncertainty component and the quantities $\partial f/\partial x_i$ are the partial derivatives of y, often referred to as sensitive coefficients.

Equation models for both the uncertainty calculation for scale realisations and comparisons are proposed in the following paragraphs 3.1 and 3.2.

3.1 Equation models for the scale realisations

By referring to the different uncertainty components reported in the tables, the general equation (20) may be adopted where N denotes the number of doubling steps in the non-linearity measurement and c_{19} converts the current uncertainty into temperature. Specific equations for the different calibration schemes are obtained by including the appropriate uncertainty components $u(x_i)$, according to Table A.

$$u_c^2(\lambda,T)_{scale} = \left[u(x_1)^2 + u(x_3)^2 + u(x_4)^2 + u(x_5)^2 + u(x_{20})^2\right]\left(\frac{T}{T_{ref}}\right)^4 + \left[u(x_6)^2 + u(x_7)^2 + u(x_8)^2 + u(x_9)^2 + u(x_{10})^2 + u(x_{11})^2 + u(x_{12})^2\right]\left(\frac{T}{\lambda}\right)^2\left(\frac{T}{T_{ref}} - 1\right)^2 +$$

$$+\left[u(x_2)^2 + u(x_{13})^2 + N^2u(x_{14})^2 + u(x_{15})^2 + u(x_{16})^2 + u(x_{17})^2 + u(x_{18})^2 + u(x_{22})^2\right]\left(\frac{\lambda T^2}{c_2}\right)^2 + c_{19}^2u(x_{19})^2 + u(x_{21})^2 + u(x_{23})^2 \qquad (20)$$

The following **Table C** summarises the uncertainty components in the realisation of the ITS-90. According to the classification reported in [29], two categories of uncertainty are introduced, i.e., a) normal and b) best, referring to uncertainties that a) can be easily obtained at present in national metrology institutes, b) can be obtained with considerable effort by the small number of leading workers in the field. It is worth to note that not all the components in Table C apply for all the three realisation schemes. The dominant contributions (~0.1 K or more at 3000 K for the category best) are marked with a dark grey cell and are from components 6, 10 and 14 for all three schemes and in addition, from component 20 for scheme 1.

TABLE C Values for uncertainty components $u(x_i)$ and uncertainty contributions $u_i(y)$, all for k=1

No *i*	quantity X_i	standard uncertainty $u(x_i)$		uncertainty contribution $u_i(y)$ / mK			
				at T_{ref}		at 3000 K (*)	
		normal value	best value	normal value	best value	normal value	best value
1	Impurities / mK	10	5	10	5	50	25
2	Emissivity	0.0001	$2x10^{-5}$	10	2	49	9
3	Temperature drop / mK	5	2	5	2	25	10
4	Plateau identification / mK	5	1	5	1	25	5
5	Repeatability / mK	20	5	20	5	101	25
6	Wavelength([1]) / nm	0.08	0.03	0	0	464	166
7	Reference detector / nm	0.00018	0	0	0	1	0
8	Scattering, Polarisation / nm	0.0009	0.0006	0	0	5	3
9	Repeatability of calibration / nm	0.012	0.0018	0	0	66	11
10	Drift / nm	0.12	0.03	0	0	663	166
11	Out-of-band transmittance / nm	0.015	0.002	0	0	86	11
12	Interpolation and Integration([2]) / nm	0.014	$2x10^{-5}$	0	0	83	0.1
13	SSE	0.0005	$3x10^{-5}$	44	3	220	13
14	Non-linearity ([3])	0.0003	$5x10^{-5}$	0	0	1610	268
15	Drift	0.0022	0.00011	181	9	909	45
16	Ambient conditions	0.0003	$2x10^{-5}$	24	2	122	8
17	Gain ratios	0.0005	0.0001	40	8	203	41
18	Repeatability	0.0001	$3x10^{-5}$	11	2	58	11
19	Current	$1.8x10^{-5}$	$1x10^{-5}$	12	7	24	13
20	Drift, stability ([+]) / mK	50	20	50	20	1050	350
21	Base and ambient temperature / mK	9	2	9	2	0	0
22	Positioning	0.001	0.0002	81	16	283	56
23	Polynomial fit ([+]) / mK	50	10	50	10	100	30

(*) 2500 K for components from 19 to 23
([+]) different values for gas lamps above 1900 K
([1]) monochromator based
([2]) effective wavelength approach
([3]) number of doubling steps N = 13.2

Figure 5 shows the uncertainty behaviour for the three schemes of realisation of the ITS-90 and for the two categories, i.e., normal and best.

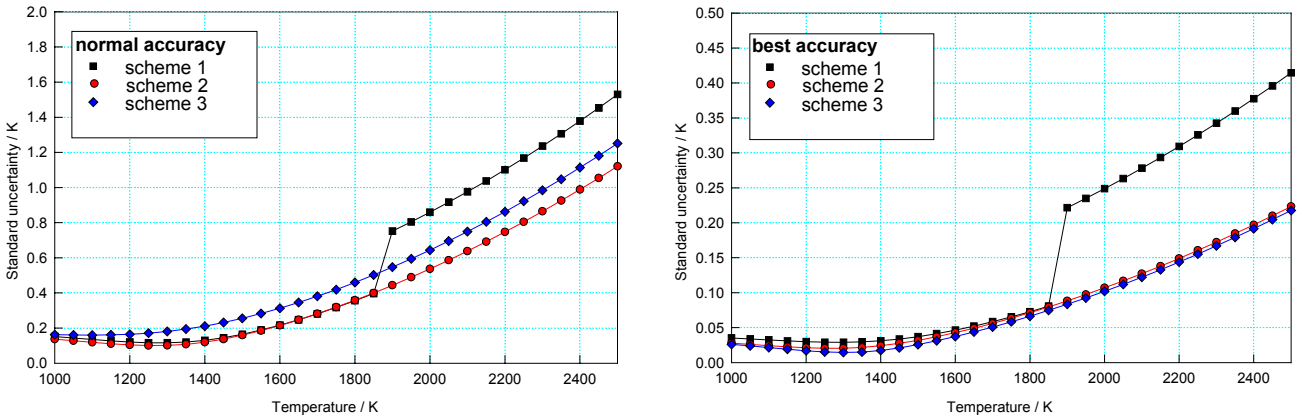

Figure 5: Standard uncertainty in the ITS-90 realisation at normal and best accuracy level

3.2 Equation models for the comparisons

An equation model for the comparisons may be obtained by adding to $u_c^2(\lambda;T)_{scale}$ the components in Table B.

$$u_c^2(\lambda,T)_{comparison} = u_c^2(\lambda,T)_{scale} + \left[u(x_{24})^2\right]\left(\frac{T}{T_{ref}}\right)^4 + \left[u(x_{25})^2 + u(x_{27})^2 + u(x_{28})^2\right]\left(\frac{\lambda T^2}{c_2}\right)^2 + u(x_{26})^2 + u(x_{29})^2 + u(x_{30})^2 + u(x_{31})^2 \quad (21)$$

References

1. Machin G, Ricolfi T., Battuello M., Negro G., Jung H.J., Bloembergen P., Bosma R., Ivarsson J., Weckstrom T., *Metrologia*, 1996, **33**, 197-206
2. Sakuma F., Sakate H., Johnson B.C., Gibson C., Machin G., Ricolfi T., Battuello M., Fischer J., Jung H.J., *Metrologia*, 1996, **33**, 241-248
3. CCT KC-5: *Comparison of local realisation of the ITS-90 between the silver point and 1700 °C using vacuum tungsten-strip lamps as transfer standards*. The elaboration of the results of this intercomparison is currently in progress.
4. Preston-Thomas H., *Metrologia*, 1990, **27**, 3-10; 107.
5. Fischer J., Jung H.J., *Metrologia*, 1989, **26**, 245-252
6. Bongiovanni G., Crovini L., Marcarino P., *Metrologia*, 1975, **11**, 125-132
7. Ricolfi T., Lanza F., *High Temp.-High Press.*, 1977, **9**, 483-487
8. Mangum, B.W., Bloembergen P., Fellmuth B., Marcarino P., Pokhodun A.I., *Document CCT99-11*
9. Jung H.J., Inst. Phys. Conf. Ser. No. 26, 1975, 278-286
10. McEvoy, H., Machin, G., *Report on the thermal conductivity of graphite*, produced for CCT WG5, 2001, 11 pp.
11. Battuello M., Ricolfi T., Wang L., *Document CCT/2000-1 of the 20th Meeting of the CCT*, Paris, 2000
12. Anderson V.E., Fox N.P., Nettleton D.H., *Applied Optics*, 1992, **31**, 536-545
13. Rosso A, Righini F, *Measurement*, 1985, **3**, 131-136
14. Hamamatsu Technical Data Sheet
15. Jung H.J., *Metrologia*, 1986, **23**, 19-31
16. Peter Saunders, *Uncertainty arising from the use of the mean effective wavelength in realising ITS-90*, to be published in TMCSI, 2002
17. Machin, G., Sergienko, R., *Proc. TEMPMEKO 2001*, (Edited by B. Fellmuth, J. Seidel, G. Scholz), VDI-Verlag, Berlin, 2002, 155-160
18. Battuello, M., Ricolfi, T., *TRIRAT Project-Report on the comparison of local temperature scales with transfer infrared thermometers in the medium-temperature range*
19. Matveyev, M. S., private communication
20. *Data supplied by the participants to the CCT-K5*
21. Fischer, J., e-mail of September 24, 2001 to M. Battuello on “SSE correction at PTB”
22. Ballico, M. J., *Independent Australian Realization of the International Temperature Scale of 1990 using the recommissioned APEP2 pyrometer*, CSIRO Technical Memorandum No. TIP-P48, 1997, 34 pp.
23. Clare, J. F., Meas. Sci. Technol. 2002, **13**, N38-N41
24. Yuan, Z., e-mail of September 28, 2001 to M. Battuello on “SSE correction at NIM”
25. Matveyev, M.S., *Proc. TEMPMEKO 2001*, (Edited by B. Fellmuth, J. Seidel, G. Scholz), VDI-Verlag, Berlin, 2002, 167-171
26. Fischer J., Hartmann J., *Proc. TEMPMEKO ’99*, (Edited by J.D. Dubbeldam and M.J. De Groot), NMi-VSL, Delft, 1999, 561-566
27. *Protocol to the Comparison of local realisations of the ITS-90 between the silver Point and 1700 °C using Vacuum Tungsten-Strip Lamps as Transfer Standards*
28. *Guide to the Expression of Uncertainty in Measurement*, Geneva, International Organisation for Standardisation, 1993, 101 pp.
29. Jung H.J., *Proc. TEMPMEKO ’96*, (Edited by P. Marcarino), Levrotto & Bella, Torino, 1997, 235-244